EAI Endorsed Transactions
on ______________________________

Research Article [redacted]

A Pervasive Sensing Approach to Automatic Assessment of Trunk Coordination Using Mobile Devices

Zilu Liang[1,4,*], Yasuyuki Yoshida[2], Nami Iino[2], Takuichi Nishimura[2], Mario Alberto Chapa-Martell[3], and Satoshi Nishimura[2]

[1]Kyoto University of Advanced Science, Kyoto, Japan
[2]National Institute of Advanced Industrial Science and Technology, Tokyo, Japan
[3]CAC Corporation, Tokyo, Japan
[4]The University of Tokyo, Tokyo, Japan

Abstract

Assessing trunk coordination has many potential applications in health promotion. However, traditional bio-mechanical approaches are not suited for daily use as they require expensive devices and manual analysis. This study aimed to develop an approach for automatic classification of good and poor trunk coordination using widely available mobile devices. We investigated different combinations of sensor locations (i.e. chest and pelvis), sensing modalities (i.e. accelerometer and gyroscope) and classification techniques (i.e. SVM, KNN, and decision tree). Results showed that using both sensing modalities at chest and pelvis with SVM produced the best classification accuracy: 96% for chest rotation and 100% for pelvis rotation. In practice, however, using one device with both sensing modalities (i.e. accelerometer and gyroscope) will achieve a better trade-off between feasibility and accuracy. In this case, the device should be fixed on the chest. KNN should be selected as the classification technique for chest rotation (best accuracy 95%), and SVM should be selected as the classification technique for pelvis rotation (best accuracy 79%). Post hoc analysis found that poor coordination during chest rotation was associated to weak cross-correlation of angular velocity between chest and pelvis in the frontal plane, while poor coordination during pelvis rotation was associated to weak correlations of angular velocity between the three orthogonal components at chest. This study demonstrated how simple mobile devices can capture relevant motion data and extract key features that help construct computational models for automatic assessment of trunk coordination.

Keywords: trunk coordination; health promotion; pervasive computing; inertia measurement units (IMU); accelerometer; gyroscope; machine learning.

Received on 28 August 2018, accepted on 14 July 2019, published on 22 July 2019

doi: 10.4108/_______________

[*]Corresponding author. Email:z.liang@cnl.t.u-tokyo.ac.jp

1. Introduction

Trunk strength is critical for the prevention of lower back pain and fall accident in elderly population [1, 2]. Whereas people tend to equate trunk strength with the strength of trunk muscles, there is increasing evidence that the coordination of muscles, joints and ligaments is even more important in providing sufficient trunk strength and is yet not strongly associated to trunk muscle strength [3, 4]. Moreover, impaired coordination was found to be associated to many sickness including low back pain [5-7], stroke [8], and unilateral vestibular hypofunction [9]. To this end, trunk coordination ability can be used as an indicator of a person's physical health. Nevertheless, there is no tool supporting the assessment of dynamic coordination ability of trunk in daily life settings. Trunk coordination has mainly been studied in low back pain research [2, 5-7, 10-15]. Traditional approaches require the use of complicated and expensive motion analysis systems that can only be used in laboratories [5, 11]. It is not feasible to apply the same approaches to daily life settings.

This study aimed to develop an approach for automatic nominal assessment of trunk coordination ability using mobile devices. We sought for solutions at the intersection of pervasive sensing and machine learning, so that our methods could benefit anyone who has simple mobile devices such as smartphones, iPod and iPad. The accelerometers and gyroscopes embedded in these devices have enabled data-driven and ubiquitous approaches for motion tracking and analysis in free-living conditions [9, 16-21]. These portable sensors allow for capturing motion data in all three planes of motion (i.e. sagittal plane, frontal plane, and transverse plane) and is thus suited for the analysis of trunk coordination [11]. We have previous experimented with other types of portable devices such as Nintendo Wii Board but failed to achieve high accuracy [22]. Our study differed from the previous studies in that we addressed the key issue of automating the assessment of coordination through machine learning based modelling. Machine learning has been widely used in health-related ubiquitous computing applications [21, 23-26]. The black-box approach enables us to model the complicated and high-dimensional relationships between features extracted from motion data and trunk coordination ability.

This study was conducted in three steps. We first defined two standard moves, i.e. chest rotation and pelvis rotation. These moves require smooth trunk-pelvis coordination and are easy to perform by the general population. Different from traditional biomechanical approaches that use static discrete tasks, we designed two continuous dynamic moves that provide spatial-temporal information to quantify trunk coordination.

Second, we conducted a data collection trial with a cohort of 21 participants. Two iPods with embedded accelerometers and gyroscopes were fixed on chest and on the back of pelvis to collect motion data. All moves were video recorded with the consent from participants. Since it is hard to obtain the ground truth of coordination ability, we chose to rely on the wisdom of experts. Three sports judges separately rated all the moves, and the majority of the three ratings for each move was used as the final label. The obtained datasets were split into training sets and testing sets for the machine learning process in the next step.

Third, we applied three machine learning techniques, i.e. support vector machine (SVM), k-nearest neighbour (KNN) and decision tree, to train the classification models. The performance of the classifiers was evaluated using four metrics: *sensitivity*, *specificity*, *accuracy* and *balanced accuracy*. We also investigated the effect of sensor location and sensing modality, and we identified the motion patterns indicating poor coordination through post hoc statistical analysis.

Our analysis revealed that using two devices (one fixed on the chest and the other fixed on the back of the pelvis) with SVM chosen as the machine learning technique produced the best classification accuracy on trunk coordination ability, i.e. 96% for chest rotation and 100% for pelvis rotation. In real situation, however, using one device with both sensing modalities (i.e. accelerometer and gyroscope) will achieve a better trade-off between feasibility and accuracy. In this case, the device should be fixed on the chest. KNN should be selected as the classification technique for chest rotation (best accuracy 95%), and SVM should be selected as the classification technique for pelvis rotation (best accuracy 79%) respectively. Post hoc analysis found statistically significant differences between good and poor coordination on the top five features. Poor coordination during chest rotation was associated to lower values of the maximal cross-correlation (y component), the mean (x component at pelvis), and the fifth fast Fourier transform (FFT) coefficient (y component at chest) of angular velocity, while poor coordination during pelvis rotation was associated to weaker correlations between the x and the y components, weaker correlations between the x and the z components, and weaker covariance between the x and the z component of the angular velocity of chest. We may infer that judges used different strategies in assessing coordination ability through the two standard moves. For chest rotation, attention was given to the movement of both chest and pelvis and their coordination. For pelvis rotation, attention was dominantly paid to the coordination of chest in three orthogonal directions.

This study demonstrated how simple mobile devices can capture relevant motion data and extract key features that help construct computational models for the automatic assessment of trunk coordination. The main contributions of this study are three-fold: (1) we developed a machine learning based pervasive sensing approach using widely available mobile devices; (2) we examined a number of combinations of sensor locations, sensing modalities and machine learning techniques and identified the best combinations; (3) we interpreted the machine learning models to understand the key features that characterise poor trunk coordination.

The rest of the paper is organized as follows. Section 2 provides a literature review on trunk coordination and mobile sensors for human movement analysis. Section 3 presents two standard moves, data collection protocol, and data analysis and modelling techniques. Performance evaluation of the classification models is presented in Section 4. We discuss the implication of the results within the landscape of previous studies in Section 5. The paper is concluded in Section 6.

2. Related Work

2.1. Trunk Coordination

Trunk coordination is an important aspect of trunk strength [27, 28] and has been intensively studied in low back pain research [2, 5-7, 10-15]. Different types of coordination have been investigated in previous studies, including head-trunk coordination [9], arm-trunk coordination [8], trunk-pelvis coordination [11, 13, 15], and trunk-lower limb coordination [29].

These studies focused on identifying kinematic differences in motions between individuals with pathological conditions and healthy individuals. Differences were found between normal group and low back pain group in average angle of flexion and average cycle velocity during dynamic trunk motion [12] and in the range of motion, velocity and acceleration during free dynamic oscillatory bending motion [30]. Coordination analysis demonstrates a reduction in relative motion between the pelvis and trunk in low-back-pain group at varied walking and running speed [5, 6, 11]. Moreover, trunk-pelvis was more in-phase for individuals with low back pain than those without low back pain [14].

Previous studies also illustrate the importance of evaluating all three planes of motion (i.e. sagittal plane, frontal plane and transverse plane as shown in Figure 1) simultaneously when studying trunk coordination [11, 31-33], as the spine is a complex structure exhibiting multi-axial motion during trunk rotational activities [34]. Indeed, the reduced ability to modulate coordination for pathological individuals was found both in frontal plane [11] and in transverse plane [11, 15].

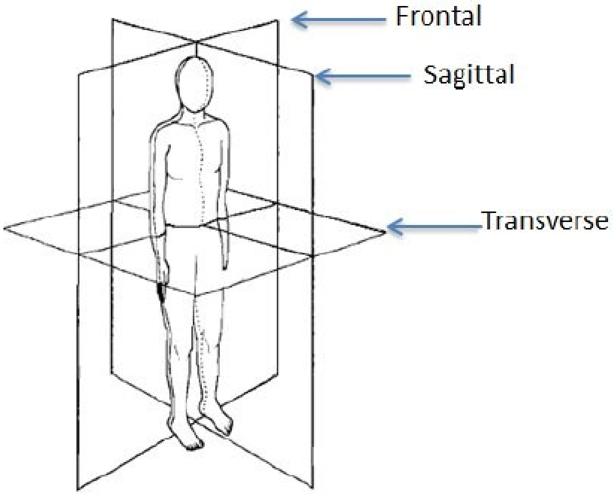

Figure 1. Cardinal planes of motion [35].

Quantitative assessment of trunk coordination has been an important topic in sport science and rehabilitation. While traditional biomechanical assessment of motion has typically used discrete measures such as peak excursions and forces, studies on coordination have mostly relied on continuous measures such as continuous relative phase (CRP) [11, 36-38]. In addition, coordination variability defined as the difference between cycle standard deviation of CPR may be an effective indicator of motion quality and pathological conditions such as low back pain [7, 39, 40]. Previous studies have found decreased coordination variability in people with low back pain compared to healthy individuals [7].

Whereas the kinematic differences in trunk coordination between pathological and healthy individuals has been intensively studied, it remains unknown as to the differences between healthy individuals with good and poor coordination. The latter is an important topic to investigate because it produces insights into the prediction and the prevention of motor diseases such as low back pain and balance impairment. Hence, this study set out to fill in the knowledge gap by establishing a novel pervasive sensing approach to the automatic assessment of good and poor coordination among health people.

2.2. Mobile Sensors in Human Movement Analysis

Human motion analysis aims to quantitatively assess motor functions and motor abilities [41]. Traditional motion analysis relies on the use of optoelectronic systems (i.e. motion capture systems) that measure the kinematics and kinetics of body joints, which requires bulky and expensive equipment and can only be conducted in laboratory settings [42]. Technology advances in recent years has seen the rise of alternative measurement techniques using mobile sensors such as accelerometers and gyroscopes. These devices have multiple advantages, including low cost, light weight, and supporting pervasive measurement even in daily life settings [43].

A set of a mutually aligned three-orthogonal accelerometer and gyroscope is generally referred to as an inertial measurement unit (IMU). An IMU is widely available in modern portable devices such as smartphones and surfaces, making it easy to measure three-dimensional linear acceleration and angular velocity in daily life [16]. The accuracy and reliability of IMU has also been validated [44]. Many studies have used IMU for gait analysis [18, 45, 46]. Studies have examined people's the ability of maintaining upright balance during walking [47], step wise repeatability [48], gait resilience to external and internal perturbations [49], and the risks of fall [50]. Previous studies also identified various key metrics [51]. In the time domain, acceleration root mean square or standard deviation are the validated metrics for balance assessment [52]. In the frequency domain, the harmonic ratio (HR) is a valid metric for assessing the symmetry and rhythm of movements [53, 54], and the relative power of the first signal harmonic with respect to the total power of the signal is used to access the smoothness of gait [55].

Another important area using mobile sensors is the detection of daily activities [56-61] and sleep [23, 24, 62-65]. The main purposes include the detection of different types of activities in daily life, the modelling of daily activity patterns, the detection of sleep stages throughout a night, and the promotion of physical activities and sleep hygiene. This line of research has many applications to health promotion [20, 66, 67], rehabilitation [19, 68, 69] and sports training [70]. While it is relatively easy to distinguish among different postures such as sitting, standing, lying or motor activities [71, 72], quantifying the amount of

movements of thorax and pelvis respectively. Previous studies have demonstrated the validity of these locations in studying motor control [10, 82-84].

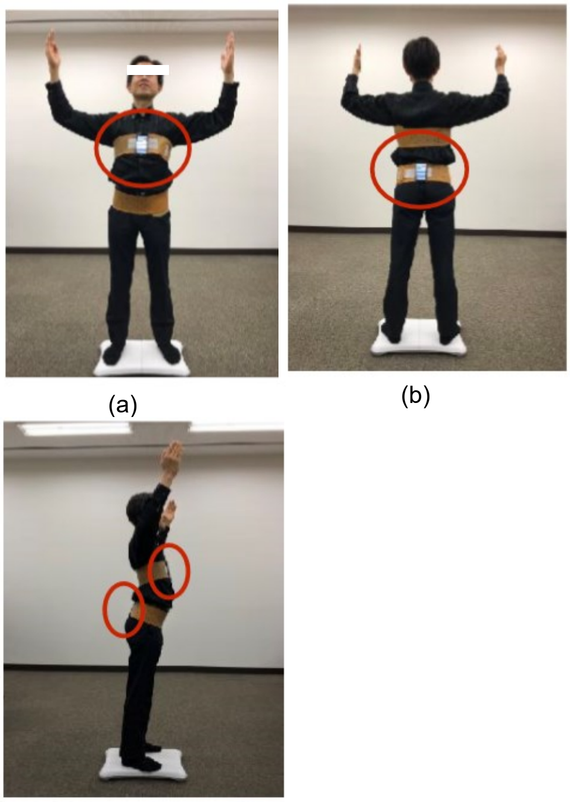

Figure 3. Sensor location in data collection trial: (a) front view; (b) back view; (c) side view. The two iPods were fixed on the chest and on the back of pelvis respectively using belts.

These two iPods were denoted as $\mathrm{iPod}^{\mathrm{ch}}$ and $\mathrm{iPod}^{\mathrm{pel}}$ respectively. Each iPod has an embedded triaxial accelerometer and a triaxial gyroscope. These sensors enabled the iPods to measure acceleration and angular velocity in three orthogonal directions. The sampling frequencies of both sensing modalities were 50Hz, and the dynamic range of the accelerometer was $\pm$2.3g. The devices were rigidly fixed to the body segments using belts, with the sensors' reference system aligned with the anatomic axes of the segments where the sensors were attached. To make sure that data collected by the two iPods were aligned in time, we linked the two devices to a third iPod using a mobile application named Axis Visualizer that we developed in our previous study [85]. With the Axis Visualizer opened on all three iPods, we could start the measurement of $\mathrm{iPod}^{\mathrm{ch}}$ and $\mathrm{iPod}^{\mathrm{pel}}$ at exactly the same time by simply tapping the start button on the third iPod.

Measurement Protocol and Labelling

As is shown in Figure 3, the two iPods were fixed on the chest and on the back of the pelvis using belts. Participant was instructed to perform the standard moves by following the demo video (available at https://www.youtube.com/watch?v=7cx4KX3JpMQ). The data collection trial had three sessions. Each session consisted of performing chest rotation for 12 seconds and pelvis rotation for 12 seconds. Participants started with relaxing and adjusting the standing posture, followed by performing the three sessions with a 10-second rest between sessions. All movements were video recorded.

After the trial, the videos were shown to three sports judges for rating. The rating was done independently, i.e. all judges were not aware of each other's assessment. The final rating was obtained using the following rule: a move was labelled as 1 only when at least two judges rate it as 1 (= poor coordination); or else the move was labelled as 0 (= good coordination).

3.3. Data Analysis and Modelling Techniques

Data from all the participants were used in the final analysis. Since the iPods collected raw data of acceleration and angular velocity in three planes of motion, the following 4 datasets were obtained for each standard move. In the following equations, $\boldsymbol{a}_X$, $\boldsymbol{a}_Y$, $\boldsymbol{a}_Z$ denote the x, y, and z components of acceleration, and $\boldsymbol{\omega}_X$, $\boldsymbol{\omega}_Y$, $\boldsymbol{\omega}_Z$ denote the x, y, and z components of angular velocity.

- Dataset $\boldsymbol{A}^{ch}$ comprised the acceleration data in three orthogonal directions and the root sum of squares (RSS) collected by the accelerometer in $\mathrm{iPod}^{\mathrm{ch}}$.

$$\boldsymbol{A}^{ch} = \{\boldsymbol{a}_X^{ch}, \boldsymbol{a}_Y^{ch}, \boldsymbol{a}_Z^{ch}, \boldsymbol{a}_{RSS}^{ch}\} \tag{1}$$

$$\boldsymbol{a}_{RSS}^{ch} = \sqrt{(\boldsymbol{a}_X^{ch})^2 + (\boldsymbol{a}_Y^{ch})^2 + (\boldsymbol{a}_Z^{ch})^2} \tag{2}$$

- Dataset $\boldsymbol{A}^{pel}$ comprised the acceleration data in three orthogonal directions and the RSS collected by the accelerometer in $\mathrm{iPod}^{\mathrm{pel}}$.

$$\boldsymbol{A}^{pel} = \{\boldsymbol{a}_X^{pel}, \boldsymbol{a}_Y^{pel}, \boldsymbol{a}_Z^{pel}, \boldsymbol{a}_{RSS}^{pel}\} \tag{3}$$

$$\boldsymbol{a}_{RSS}^{pel} = \sqrt{(\boldsymbol{a}_X^{pel})^2 + (\boldsymbol{a}_Y^{pel})^2 + (\boldsymbol{a}_Z^{pel})^2} \tag{4}$$

- Dataset $\boldsymbol{\Omega}^{ch}$ comprised the angular velocity data in three orthogonal directions and the RSS collected by the gyroscope in $\mathrm{iPod}^{\mathrm{ch}}$.

$$\boldsymbol{\Omega}^{ch} = \{\boldsymbol{\omega}_X^{ch}, \boldsymbol{\omega}_Y^{ch}, \boldsymbol{\omega}_Z^{ch}, \boldsymbol{\omega}_{RSS}^{ch}\} \tag{5}$$

$$\boldsymbol{\omega}_{RSS}^{ch} = \sqrt{(\boldsymbol{\omega}_X^{ch})^2 + (\boldsymbol{\omega}_Y^{ch})^2 + (\boldsymbol{\omega}_Z^{ch})^2} \tag{6}$$

Table 1. Features and denotations in Feature Set I.

Time Domain		Frequency Domain	
Feature	Denotation	Feature	Denotation
Maximum	*maxX, maxY, maxZ, maxRSS*	First Five FFT Coefficients	*fftCoX1~5, fftCoY1~5, fftCoZ1~5, fftCoRSS1~5*
Minimum	*minX, minY, minZ, minRSS*	Principle Frequency	*prinfreqX, prinfreqY, prinfreqZ, prinfreRSS*
Mean Value	*meanX, meanY, minZ, meanRSS*	Peak Frequency	*PeakfreqX, peakfreqY, peakfreqZ, peakfreqRSS*
Standard Deviation	*sdX, sdY, sdZ, sdRSS*	Spectral Energy	*seX, seY, seZ*
Kurtosis	*kuX, kuY, kuZ, kuRSS*		
Root Mean Square	*rmsX, rmsY, rmsZ, rmsRSS*		
Median Cross Zeros	*mcX, mcY, mcZ*		
Correlation X, Y, Z	*corXY, corXZ, corYZ*		

Table 2. Features and denotations in Feature Set II.

Time Domain	
Feature	Denotation
Minimum value of cross-correlation between two iPods	*xCorMin, yCorMin, zCorMin,*
Maximum value of cross-correlation between two iPods	*xCorMax, yCorMax, zCorMax*
Lag of the minimum value of cross-correlation	*xlagMin, ylagMin, zlagMin,*
Lag of the maximum value of cross-correlation	*xlagMax, ylagMax, zlagMax*

Table 3. Feature extraction for nine methods with varied sensor locations and sensing modalities.

Methods	Sensor Location	Sensing Modality	Raw Data	Extracted Features
Single device with single modality				
Method-1	Chest	Accelerometer	$\boldsymbol{A}^{ch}$	Feature Set I
Method-2	Chest	Gyroscope	$\boldsymbol{\Omega}^{ch}$	Feature Set I
Method-3	Pelvis	Accelerometer	$\boldsymbol{A}^{pel}$	Feature Set I
Method-4	Pelvis	Gyroscope	$\boldsymbol{\Omega}^{pel}$	Feature Set I
Single device with multiple modalities				
Method-5	Chest	Accelerometer & gyroscope	$\boldsymbol{A}^{ch}$, $\boldsymbol{\Omega}^{ch}$	Feature Set I
Method-6	Pelvis	Accelerometer & gyroscope	$\boldsymbol{A}^{pel}$, $\boldsymbol{\Omega}^{pel}$	Feature Set I
Multiple devices with single modality				
Method-7	Chest, pelvis	Accelerometer	$\boldsymbol{A}^{ch}$, $\boldsymbol{A}^{pel}$	Feature Set I & II
Method-8	Chest, pelvis	Gyroscope	$\boldsymbol{\Omega}^{ch}$, $\boldsymbol{\Omega}^{pel}$	Feature Set I & II
Multiple devices with multiple modalities				
Method-9	Chest, pelvis	Accelerometer & gyroscope	$\boldsymbol{A}^{ch}$, $\boldsymbol{A}^{pel}$, $\boldsymbol{\Omega}^{ch}$, $\boldsymbol{\Omega}^{pel}$	Feature Set I & II

attention to the movement of chest in assessing coordination during pelvis rotation.

4.2. Parameter Tuning and Training

The original datasets were split into training sets (42 samples) and testing sets (21 samples). Three classification techniques (i.e. SVM, KNN, and decision tree) were applied to train classifiers for automatic classification on good and poor coordination. We obtained the optimal values of the parameters for each classification technique following the process described in 2.3.4, with 3 repetitions of 10-fold cross validation using the training sets. At each of the folds, the training set was partitioned by randomly selecting approximately 70% sample for training and 30% samples for testing. The optimal values of the parameters in the trained classifiers were selected based on the average classification accuracy over 3 repetitions, which were summarized in Table 6 (chest rotation) and Table 7 (pelvis rotation).

Table 4. Features selection in different methods for chest rotation.

Methods	Number of Selected Features	Top 5 Features
Single device with single modality (originally 65 features)		
Method-1	29	$corYZ_a^{ch}$,$fftCoY4_a^{ch}$,$peakrY_a^{ch}$,$prinfreq_a^{ch}$,$peakrRSS_a^{ch}$
Method-2	15	seX_g^{ch},sdX_g^{ch},sdX_g^{ch},$rmsX_g^{ch}$,sdZ_g^{ch},$meanZ_g^{ch}$
Method-3	12	$rmsZ_a^{pel}$,$meanZ_a^{pel}$,$meanRSS_a^{pel}$, $kuRSS_a^{pel}$, sdZ_a^{pel}
Method-4	19	mcX_g^{pel}, mcZ_g^{pel}, $covXZ_g^{pel}$, sdZ_g^{pel}, $rmsZ_g^{pel}$
Single device with multiple modalities (originally 130 features)		
Method-5	78	$fftCoZ4_g^{ch}$,$minZ_g^{ch}$, $corYZ_a^{ch}$, $covYZ_g^{ch}$, $fftCoY5_g^{ch}$
Method-6	31	$meanRSS_a^{pel}$, sdY_a^{pel}, $kuRSS_a^{pel}$, $rmsX_a^{pel}$, $rmsY_a^{pel}$
Multiple devices with single modality (originally 142 features)		
Method-7	111	$corYZ_a^{ch}$, $peakrX_a^{pel}$, $fftCoY4_a^{ch}$, $prinfreq_a^{ch}$, $peakr_a^{ch}$
Method-8	101	$yCorMax_g$, $fftCoZ4_g^{ch}$, $meanX_g^{pel}$, $zCorMax_g$, $fftCoY5_g^{ch}$
Multiple devices with multiple modalities (originally 284 features)		
Method-9	183	$yCorMax_g$, $fftCoZ4_g^{ch}$, $meanX_g^{pel}$, $zCorMax_g$, $fftCoY5_g^{ch}$

Table 5. Features selection in different methods for pelvis rotation.

Methods	Number of Selected Features	Top 5 Features
Single device with single modality (originally 65 features)		
Method-1	20	$sdRSS_a^{ch}$,$seRSS_a^{ch}$,$maxY_a^{ch}$,$corYZ_a^{ch}$, $maxRSS_a^{ch}$
Method-2	17	$rmsZ_g^{ch}$, $meanZ_g^{ch}$, $fftCoZ5_g^{ch}$, sdZ_g^{ch}, $rmsX_g^{ch}$
Method-3	11	msZ_a^{pel} , $fftCoZ5_a^{pel}$, $maxZ_a^{pel}$, sdZ_a^{pel} , $rmsX_a^{pel}$
Method-4	14	$meanZ_g^{pel}$, $fftCoZ5_g^{pel}$, $rmsZ_g^{pel}$, sdZ_g^{pel} , sdX_g^{pel}
Single device with multiple modalities (originally 130 features)		
Method-5	41	$sdRSS_a^{ch}$, $corXY_g^{ch}$, $corXZ_g^{ch}$, $seRSS_a^{ch}$, $fftCoRSS3_g^{ch}$
Method-6	68	$fftCoX3_g^{pel}$, mcX_a^{pel} , $maxRSS_g^{pel}$, $minY_g^{pel}$, $fftCoZ4_a^{pel}$
Multiple devices with single modality (originally 142 features)		
Method-7	78	$sdRSS_a^{ch}$, $seRSS_a^{ch}$, $zCorMax_a$, mcX_a^{pel} , $corYZ_a^{ch}$
Method-8	45	$corXY_g^{ch}$, $covYZ_g^{ch}$, $corXZ_g^{ch}$, $covXZ_g^{ch}$, $corYZ_g^{ch}$
Multiple devices with multiple modalities (originally 284 features)		
Method-9	111	$corXY_g^{ch}$, $zCorMax_a$, $covXZ_g^{ch}$, $sdRSS_a^{ch}$, $corXZ_g^{ch}$

SVM achieved the best cross-validation accuracy for both moves. For chest rotation, the training accuracy of SVM was generally the best among the three techniques, while decision tree was the weakest technique among the three. For pelvis rotation, SVM and KNN produced similar training performance and were both better than decision tree.

Table 7. Tuned parameters and best cross-validation accuracy of classification technique for pelvis rotation.

	SVM				KNN		Decision Tree		
	C	γ	Num of SV	Best Acc	k	Best Acc	Complexity Parameter	Split Method	Best Acc
Method-1	0.001	0.000001	20	0.76	23	0.76	0.2	Gini	0.50
Method-2	5	1	39	0.71	7	0.80	0.27	Information	0.61
Method-3	64	0.001	22	0.81	5	0.82	0.25	Gini	0.50
Method-4	100	0.0001	30	0.74	15	0.72	0.42	Gini	0.50
Method-5	4	0.01	24	0.93	5	0.83	0.44	Gini	0.50
Method-6	256	0.0001	23	0.84	5	0.83	0.25	Gini	0.50
Method-7	2	0.01	39	0.74	5	0.75	0.31	Gini	0.50
Method-8	256	0.001	20	0.91	13	0.76	0.30	Gini	0.50
Method-9	2	0.01	40	0.81	5	0.73	0.42	Gini	0.50

Table 8. Performance of classifiers for chest rotation.

	SVM				KNN				Decision Tree			
	Sen	Spe	Acc	Bal Acc	Sen	Spe	Acc	Bal Acc	Sen	Spe	Acc	Bal Acc
Method-1	0.43	1.00	0.62	0.71	0.36	1.00	0.57	0.68	0.43	0.86	0.57	0.64
Method-2	0.93	1.00	0.95	0.96	0.57	1.00	0.71	0.79	0.43	0.71	0.52	0.57
Method-3	0.58	0.67	0.62	0.63	0.83	0.56	0.71	0.69	0.33	0.78	0.52	0.56
Method-4	0.90	0.50	0.70	0.70	0.90	0.50	0.70	0.70	0.50	0.30	0.40	0.40
Method-5	1.00	0.80	0.90	0.90	1.00	0.90	0.95	0.95	0.45	0.40	0.43	0.43
Method-6	0.58	0.75	0.65	0.67	0.83	0.75	0.80	0.79	0.42	0.63	0.50	0.52
Method-7	0.46	0.63	0.52	0.54	0.61	0.75	0.67	0.68	0.31	0.50	0.38	0.40
Method-8	0.89	0.64	0.75	0.76	0.44	0.91	0.70	0.68	0.56	0.91	0.75	0.73
Method-9	0.92	1.00	0.95	0.96	0.62	0.71	0.65	0.66	0.77	0.28	0.60	0.53

Table 9. Performance of classifiers for pelvis rotation.

	SVM				KNN				Decision Tree			
	Sen	Spe	Acc	Bal Acc	Sen	Spe	Acc	Bal Acc	Sen	Spe	Acc	Bal Acc
Method-1	1.00	0.00	0.62	0.50	1.00	0.00	0.62	0.50	1.00	0.00	0.62	0.50
Method-2	0.93	0.29	0.71	0.61	0.93	0.29	0.71	0.61	0.93	0.29	0.71	0.61
Method-3	0.80	0.33	0.67	0.57	0.93	0.50	0.81	0.72	1.00	0.00	0.71	0.50
Method-4	0.93	0.17	0.71	0.55	0.87	0.17	0.67	0.52	1.00	0.00	0.71	0.50
Method-5	0.92	0.67	0.81	0.79	1.00	0.22	0.67	0.61	1.00	0.00	0.57	0.50
Method-6	1.00	0.20	0.62	0.60	1.00	0.10	0.57	0.55	1.00	0.00	0.52	0.50
Method-7	1.00	0.60	0.90	0.80	1.00	0.40	0.856	0.70	1.00	0.00	0.76	0.50
Method-8	1.00	1.00	1.00	1.00	1.00	0.14	0.70	0.57	1.00	0.00	0.65	0.50
Method-9	1.00	0.40	0.85	0.70	1.00	0.20	0.80	0.60	1.00	0.00	0.75	0.50

For chest rotation, all the features of interest were extracted from angular velocity of chest and pelvis. The WSR test showed that there were significant differences between good and poor coordination on the mean values of the following features: the maximal cross-correlation of the *y* component between chest and pelvis ($p < 0.001$), the

one feature, i.e. the maximal cross-correlation of the *y* component of the angular velocity between the chest and the pelvis. In other words, a move will be considered as an indicator of poor coordination if the previous-mentioned maximal cross-correlation is negative. In comparison, identifying and interpreting the relationships between the input features and the final classification outcomes for SVM and KNN required more complicated post-hoc analysis.

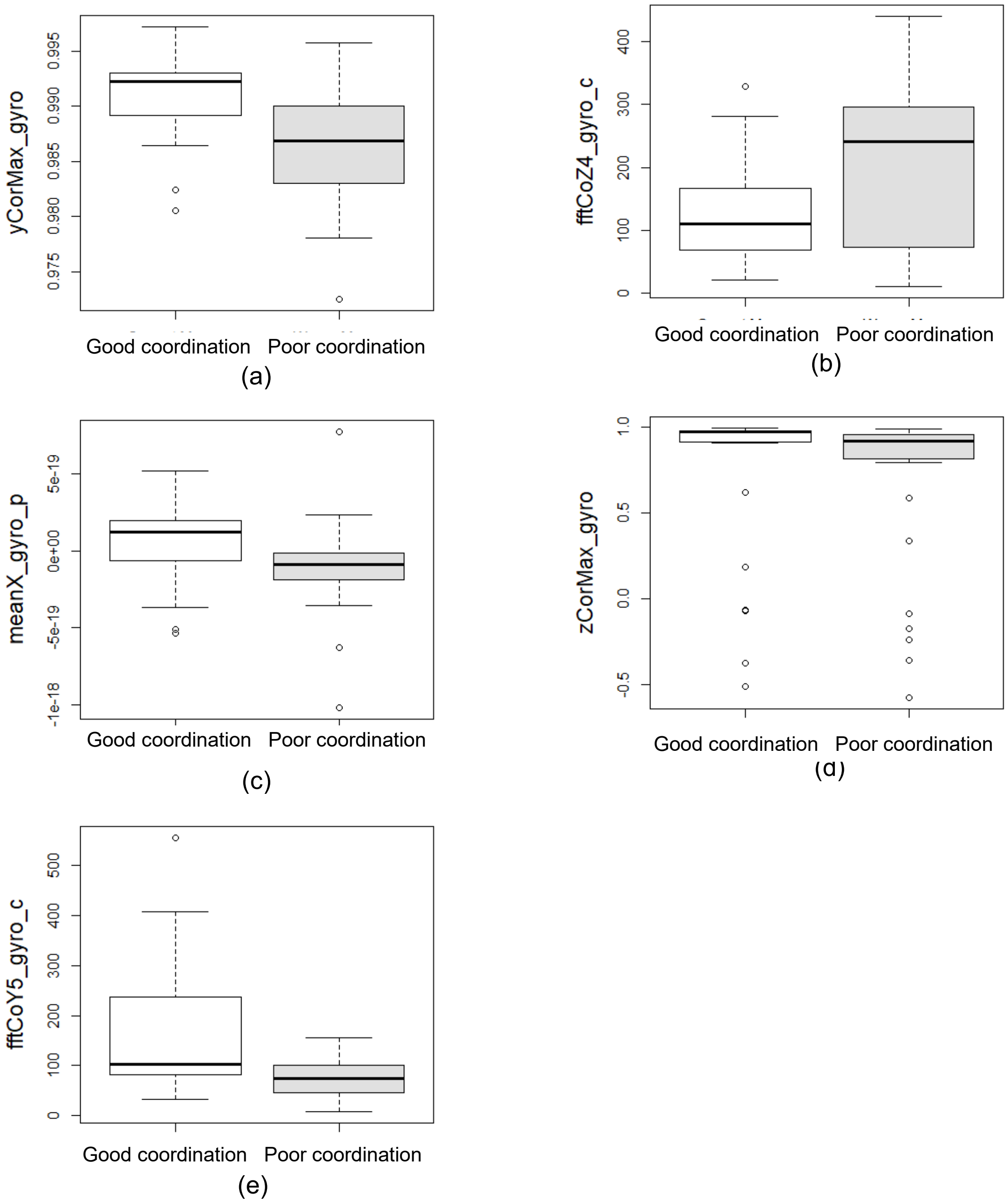

Figure 6. Box-and-Whisker plots on top five features selected in Method-9 for good and poor coordination during chest rotation: (a) maximal value of cross-correlation of y component of angular velocity between chest and pelvis; (b) fourth FFT coefficient of z component of angular velocity of chest; (c) mean value of x component of angular velocity of pelvis; (d) maximal value of cross-correlation of z component of angular velocity between chest and pelvis; (e) fifth FFT coefficient of y component of angular velocity of chest. Thick lines, bot edges and whiskers represent the median, the 25-75% quartile range and the overall range respectively.

reduced relative motion between pelvis and trunk during walking and running for people with poor coordination [5, 6, 11]. Additionally, features with strong distinguishing power were identified in three orthogonal directions, suggesting that coordination assessment should consider all three planes of motion as has been advocated in previous studies [11, 15, 31-33]. Another interesting finding was that standard deviations that were widely used to characterise movements variability were not always important features, despite of its wide use in gait studies [51]. This backs up previous findings that variability may not be a proper metrics for assessing the stability of human movement [39].

Although this study obtained promising results, there were some limitations demanding further efforts. The main limitation of this study was that we only constructed global models for the whole cohort. These models thus did not address the characteristics of different populations in terms of age, gender, and exercise habit. Second, the analysis was conducted based on the assumption that interpersonal variation and intrapersonal variation satisfied the same distribution, as the collected datasets contained multiple samples from each participant. This assumption can be eliminated when more participants were recruited in future studies.

6. Conclusions

In this study we proposed a pervasive sensing approach for automatic assessment of trunk coordination during chest rotation and pelvis rotation. We have shown that using multiple mobile devices with both sensing modalities (i.e. accelerometer and gyroscope) achieved the best accuracy in classifying trunk coordination during chest rotation (96%) and pelvis rotation (100%). SVM and KNN produced comparable performance while decision tree was the weakest classification technique. Through post hoc analysis, we found that poor coordination during chest rotation was associated to weaker coupling between chest and pelvis and lower angular velocity of the chest, and poor coordination during pelvis rotation was associated to weaker coupling between the three components of angular velocity of the chest. We also found that using single device produced comparable performance for chest rotation (95%) and slightly reduced performance for pelvis rotation (79%). Nevertheless, single-device strategy may be a good trade-off between feasibility and accuracy in practical situation. In summary, our results validated the potential of harnessing widely available mobile devices for automatic nominal assessment of trunk coordination in daily life settings.

Acknowledgements.
This study was supported by an Artificial Intelligence Research Grant from the New Energy and Industrial Technology Development Organization of Japan. We would like to thank Mr Naoki Koyama and Ms Mio Suzuki for helping with the data collection. We also appreciate the contribution of all participants to this study.

References

[1] Zimmerman, S, Greene, A, Sloane, P., et al. (2017) Preventing falls in assisted living: results of a quality improvement pilot study. *Geriatric Nursing* **38**(3):185-191.
[2] Suzuki, N. and Endo, S. (1983) A quantitative study of trunk muscle strength and fatigability in the low-back-pain syndrome. *Spine* **8**(1):69-74.
[3] Borghuis, A.J., Hof, A.L. and Lemmink, K. A. (2008) The importance of sensory-motor control in providing core stability. *Sports Medicine* **38**(11): 893-916.
[4] Cresswell, A., Oddsson, L. I. E. and Thorstensson, A. (1994) The influence of sudden perturbations on trunk muscle activity and intra abdominal pressure while standing. *Experimental Brain Research* **98**(2):336-341.
[5] Seay, J., Sauer, S., Patel, T. and Roy, T. (2016) A history of low back pain affects pelvis and trunk coordination during a sustained manual materials handling task. *Journal of Sport and Health Science* **5**(1): 52-60.
[6] Seay, J., Van Emmerik, R. and Hamill, J. (2011) Influence of low back pain status on pelvis-trunk coordination during walking and running. *Spine* **36**(16): 1070-1079.
[7] Selles, R., Wagenaar, R., Smit, T. and Wuisman, P. (2001) Disorders in trunk rotation during talking in patients with low back pain: a dynamical systems approach. *Clinical Biomechanics* **16**(3):175-181.
[8] Shaikh, T., Goussev, V., Feldman, A. and Levin, M. (2013) Arm-trunk coordination for beyond-the-reach movements in adults with stroke. *Neurorehabilitation and Neural Repair* **28**(4):355-366.
[9] Paul, S., Dibble, L., Walther, R., et al. (2017) Characterization of head-trunk coordination deficits after unilateral vestibular hypofunction using wearable sensors. *JAMA Otolaryngol Head Neck Surg* **143**(10):1008-1014.
[10] Esola, M., McClure, P., Fitzgerald, K. and Siegler, S. (1996) Analysis of lumbar spine and hip motion during forward bending in subjects with and without a history of low back pain. *Spine* **21**(1): 71-78.
[11] Seay, J., Van Emmerik, R. and Hamill, J. (2011) Low back pain status affects pelvis-trunk coordination and variability during walking and running. *Clinical Biomechanics* **26:** 572-578.
[12] McIntyre, D., Glover, L., Conino, M., et al. (1991) A comparison of the characteristics of preferred low-back motion of normal subjects and low-back-pain patients. *Journal of Spinal Disorders* **4**(1): 90-95.
[13] Sung, P. (2014) A Kinematic analysis for shoulder and pelvis coordination during axial trunk rotation in subjects with and without recurrent low back pain. *Gait & Posture* **40**:493-498.
[14] Seay, J., Van Emmerik, R. and Hamill, J. (2014) Trunk bend and twist coordination is affected by low back pain status during running. *European Journal of Sport Science* **14**(6):563-568.
[15] Smith, J. A. and Kulig, K. (2016) Trunk-pelvis coordination during turning: a cross sectional study of young adults with and without a history of low back pain. *Clinical Biomechanics* **36**:58-64.
[16] LeMoyne, R. and Mastroianni, T. (2018) The rise of inertial measurement units. *Wearable and Wireless*

falls in humans. *IEEE Transactions on Neural Systems and Rehabilitation Engineering* **19**(6):670-676.
[51] Hamacher, D., Singh, N., Van Dieen, J., et al. (2011) Kinematic measures for assessing gait stability in elderly individuals: a systematic review. *Journal of the Royal Society Interface* **8**:1682-1698.
[52] Marigold, D. and Patla, A. (2008) Age-related changes in gait for multi-surface terrain. *Gait & Posture* **27**(4):689-696.
[53] Iosa, M., Mazza, C., Pecoraro, F., et al. (2010) Control of the upper body movements during level walking in patients with facioscapulohumeral dystrophy. *Gait & Posture* 31(1):68-72.
[54] Cappozzo, A. (1982) Low frequency self-generated vibration during ambulation in normal men. *Journal of Biomechanics* **15**:8.
[55] Mazza, C., Iosa, M., Pecoraro, F. and Cappozzo, A. (2008) Control of the upper body accelerations in young and elderly women during level walking. *Journal of NeuroEngineering and Rehabilitation* **5**:30.
[56] Kan, Y.-C. and Chen, C.-K. (2012) A wearable inertial sensor node for body motion analysis. *IEEE Sensors Journal* **12**(3):651-657.
[57] Cheng, J., Amft, O., Bahle, G. and Lukowicz, P. (2013) Designing sensitive wearable capacitive sensors for activity recognition. *IEEE Sensors Journal* **13**(10):3935-3947.
[58] Stikic, M., Larlus, D., Ebert, S. and Schiele, B. (2011) Weakly supervised recognition of daily life activities with wearable sensors. *IEEE Transactions on Pattern Analysis and Machine Intelligence* **33**(12): 2521-2537.
[59] Ayzenberg, Y. and Picard, R. W. (2014) FEEL: a system for frequent event and electrodermal activity labelling. *IEEE Journal of Biomedical and Health Informatics* **18**(1): 266-277.
[60] Wu, W., Bui, A. A., Batalin, M. A., et al. (2007) Incremental diagnosis method for intelligent wearable sensor systems. *IEEE Transactions on Information Technology in Biomedicine* **11**(5): 553-562.
[61] Hegde, N., Bries, M., Swibas, T., et al. (2018) Automatic recognition of activities of daily living utilizing insole-based and wrist-worn wearable sensors. *IEEE Journal of Biomedical and Health Informatics* **22**(4): 979-988.
[62] Liang, Z. and Chapa-Martell, M. A. (2019) Accuracy of Fitbit wristbands in measuring sleep stage transitions and the effect of user-specific factors. JMIR Mhealth Uhealth 7(6): e13384.
[63] Liang, Z. and Chapa-Martell, M. A. (2019) Combining numerical and visual approaches in validating sleep data quality of consumer wearable wristbands. In Proceedings of International Workshop on Information Quality and Quality of Service for Pervasive Computing, Kyoto, Japan.
[64] Liang, Z. Ploderer, B., Chapa-Martell, M. A. (2017) Is fitbit fit for sleep-tracking?: sources of measurement errors and proposed countermeasures. In *Proceedings of the 11th EAI International Conference on Pervasive Computing Technologies for Healthcare*, 476-479, Barcelona, Spain.
[65] Liang, Z. and Chapa-Martell, M. A. (2018) Validity of consumer activity wristbands and wearable EEG for measuring overall sleep parameters and sleep structure in free-living conditions. Journal of Healthcare Informatics Research 2 (1-2):152-178.
[66] Cooper, A., Page, A., Fox, K. and Mission, J. (2000) Physical activity patterns in normal, overweight and obese individuals using minute-by-minute accelerometry. *Eur J Clin Nutr* **54**(12): 887-894.
[67] De Bruin, E. D., Hartmann, A., Uebelhart, D., et al. (2008) Wearable systems for monitoring mobility-related activities in older people: a systematic review. *Clin Rehabil* **22**:878-895.
[68] Hobert, M., Maetzler, W., Aminian, K. and Chiari, L. (2014) Technical and clinical view on ambulatory assessment in Parkinson's disease. *Acta Neurologica Scandinavica* **130**(3): 139-147.
[69] Haeuber, E., Shaughnessy, M., Forrester, L., et al. (2004) Accelerometer monitoring of home- and community-based ambulatory activity after stroke. *Archives of Physical Medicine and Rehabilitation* **85**(12): 1997-2001.
[70] Hinton-Lewis, C., McDonough, E., Moyle, G. and Thiel, D. (2016) An assessment of postural sway in ballet dancers during first position, releve and saute with accelerometers. *Procedia Engineering* **147**:127-132.
[71] Mathie, M., Coster, A., Lovell, N. and Celler, B. (2004) Accelerometry: providing an integrated, practical method for long-term, ambulatory monitoring of human movement. *Physiological Measurement* **25**(2): R1-20.
[72] Veltink, P. H., Bussmann, H. B., De Vries, W., et al. (1996) Detection of static and dynamic activities using uniaxial accelerometers. *IEEE Transactions on Rehabilitation Engineering* **4**(4): 375-385.
[73] Trost, S. G., Fees, B. S., Haar, S. J., et al. (2012) Identification and Validity of Accelerometer Cut‐Points for Toddlers. *Obesity* 20(11):2317-2319.
[74] Freedson, P., Pober, D. and Janz, K. F. (2005) Calibration of accelerometer output for children. *Med Sci Sports Exerc* **37**: S523-530.
[75] Fischer, C., Yildirim, M., Salmon, J. and Chinapaw, M. J. (2012) Comparing different accelerometer cut-points for sedentary time in children. *Pediatric Exercise Science* **24**:220-228.
[76] Kim, Y., Beets, M. W. and Welk, G. J. (2012) Everything you wanted to know about selecting the “right” Actigraph accelerometer cut-points for youth, but…: A systematic review. *Journal of Science and Medicine in Sport* **15**(4): 311-321.
[77] Hickey, A., Newham, J., Slawinska, M., et al. (2016) Estimating cut points: a simple method for new wearables. *Maturitas* **83**:78-82.
[78] Matthew, C. E. (2005) Calibration of accelerometer output for adults. *Med Sci Sports Exerc* **37**: S512-522.
[79] Dijkstra, B., Kamsma, Y. and Zijlstra, W. (2010) Detection of gait and postures using a miniaturized triaxial accelerometer-based system: accuracy in patients with mild to moderate Parkinson's disease. *Archives of Physical Medicine and Rehabilitation* **91**(8): 1272-1277.
[80] Molt, R. W., Snook, E. M., Agiovlasitis, S. and Suh, Y. (2009) Calibration of accelerometer output for ambulatory adults with multiple sclerosis. *Archives of Physical Medicine and Rehabilitation* **90**(10): 1778-1784.
[81] Nero, H., Wallen, M. B., Franzen, E., et al. (2015) Accelerometer cut points for physical activity assessment of older adults with Parkinson's disease. *PLoS One* **10**(9): e0135899.
[82] Bourke, A., O'Donovan, K. and OLaighin, G. (2008) The identification of vertical velocity profiles using an inertial sensor to investigate pre-impact detection of falls. *Medical Engineering & Physics* **30**:937-946, 2008.
[83] Klenk, J., Becker, C., Lieken, F., et al. (2011) Comparison of acceleration signals of simulated and real-world backward falls. *Med Eng Phys* **33**:368-373.